

Forced Flow Dryout Heat Flux in a Stratified Debris Bed

Jong Hee Cha, Moon Ki Chung and Yong Suk Jin

Korea Advanced Energy Research Institute

(Received March 31, 1988)

성층 데브리층에서의 강제대류 드라이아웃 열유속

차종희 · 정문기 · 진용석

한국에너지연구소

(1988. 3. 31 접수)

Abstract

The purpose of this work is to obtain the experimental data for the forced flow dryout heat flux in a heat generating stratified debris bed which simulates the degraded nuclear reactor core after severe accident. The present observations were mainly focused on the effect of coolant mass flux on the dryout heat flux in the stratified debris bed which consists of several layers with selected particle sizes under constant bed depth and temperature of inlet coolant flow conditions. The following results were obtained from this experimental work: (1) The dryout heat flux in the stratified debris bed increases with increase of upward forcing mass flux of coolant. The similar trend of increase rate of dryout heat flux in the stratified bed was observed in the uniform particle size bed. (2) For the comparison of theoretical values and experimental data, the use of surface area mean diameter as a particle diameter was suitable for the calculation of dryout heat flux.

요 약

이 연구의 목적은 가혹한 사고후 손상된 원자로심을 모의한 열이 발생하는 성층 데브리층에서의 강제대류 드라이아웃 열유속 자료를 실험적으로 얻고자 한 것이다. 여기서는 일정한 층의 깊이와 냉각재 유입온도 조건하에서 선정된 몇가지 크기의 입자로 성층을 형성한 데브리층에서 주로 냉각재 질량유속이 드라이아웃 열유속에 미치는 영향을 관찰하였다. 이 실험적 연구로부터 얻은 주요 결과는 다음과 같다. (1) 성층 데브리층에서의 드라이아웃 열유속은 질량유속의 증가와 더불어 증가하며 그 증가의 경향은 크기가 균일한 입자층에 대한 것과 유사하다. (2) 이론치와 실험치와의 비교에서 입자직경으로는 표면적 평균 직경을 사용하는 것이 적합하다.

1. Introduction

In the severe accident of a light water reactor

wherein the emergency core cooling system fails, the core could melt and be converted to a debris bed as a result of molten-fuel-coolant interaction.

The mitigation of such an accident depends on

the coolability of heat generating debris bed. At a given particle density in the degraded core, large particles will settle faster, thus a stratified bed forms with gradually decreasing particle size from the bottom to the top of the bed. Consequently, a systematic study of dryout with a stratified debris bed is required.

Concerning the dryout heat flux in the stratified or mixture bed, there were a couple of previous works. Squarer, Pieczynski, and Hochreiter¹⁾ have obtained the data on dryout heat flux in the mixture bed containing particles of different sizes under pool boiling condition. It appears that their values with equivalent particle diameter are somewhat lower than other existing values for the uniform particle size. Boldt, Reed, and Schmidt²⁾ have measured the dryout heat flux in the stratified debris bed using UO_2 particles under the condition of forced flow up to 0.08 gpm as a part of DCC-3 experiment. The stratified DCC-3 debris bed consisted of two homogeneously mixed particle distribution. The lower 40 cm of the bed consists of large particle with a surface average particle diameter of 4.67 mm. The top 10 cm of the bed consisted of smaller particles with a surface area average diameter of 1.18 mm. The data on dryout

heat flux in the stratified bed of DCC-3 experiment were generally lower than the values for uniform bed. In the DCC-3 tests, the stratified configuration and the range of coolant flow rate were something limited.

The purpose of this work is to obtain qualitative information through a series of tests for forced flow dryout heat flux in a heat generating stratified debris bed that simulates a degraded nuclear reactor core.

2. Test Description

An experimental investigation has been conducted for dryout heat flux in an inductively heated stratified debris bed with upward forced flow under atmospheric pressure. The main parts of the experimental setup are the test loop which is included debris bed, high frequency induction heater with a work coil, and related instruments. The test loop consists of a pyrex glass tube filled with steel particles, a reservoir containing distilled water, a centrifugal pump, a heat exchanger, a flow meter and piping. A schematic diagram of test loop is shown in Figure 1.

The data were obtained when carbon steel

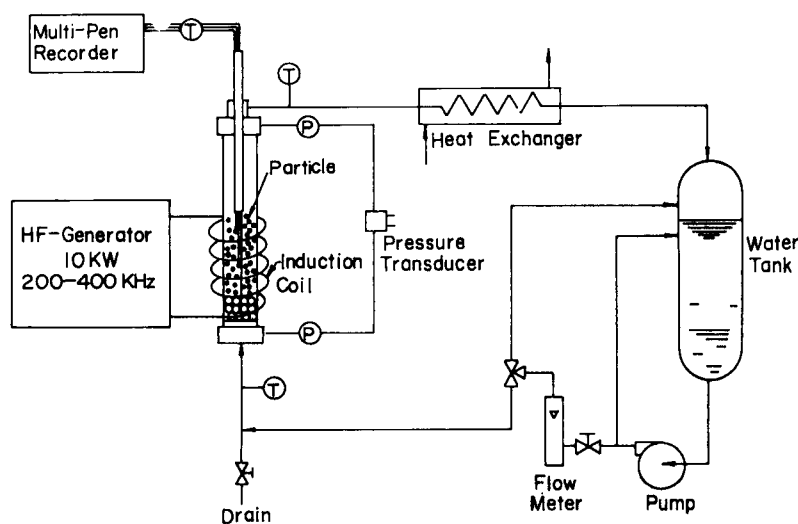


Fig. 1. Schematic Diagram of Test Loop

particle layers were placed (large particles on the bottom and small particles on the top) in a 55 mm i.d. pyrex glass column and inductively heated by passing radio-frequency current through a multi-ture work coil encircling the column. The work coil was powered by a 10 kW power output and 200 to 450 kHz high frequency generator. Carbon steel particles in the bed are supported by a stainless steel screen at the bottom of the test section. Size of the screen opening was 0.25 mm, or 60 mesh. The stainless steel reservoir tank containing 350 liters of distilled water at room temperature is connected to the inlet of the pyrex tube through a 0.5 HP centrifugal pump.

Distilled water was supplied as a coolant in the tests with mass flux variations from 0 to $3.5 \text{ kg/m}^2 \cdot \text{s}$, while maintaining a bed height and coolant inlet temperature of 110 mm and 13°C , respectively. The range of above mass flux can sufficiently cover the flow rate of the safety injection in PWR system. Subcooled coolant flows up through the particulate bed via flow meter by a pump. The coolant outflow from the bed returned to reservoir after condensation through the heat exchanger.

The instrumentation consists of the thermocouples with multipen X-Y recorder for measuring temperatures, rotameter for measuring the flow rate of coolant. The temperature at different locations in the bed was measured by using gage number 30 chromel-alumel thermocouples which were carried in thin alumina capillary tubes and connected to a multipen recorder as shown in Figure 2. Experimental errors involved in the measurements were estimated at $\pm 2\%$ for the flow rate in rotameter, and $\pm 5\%$ for reading of power input.

Prior to each run the selected particles were rinsed using acetone more than three times and shaken vigorously during rinsing. The washed and dried particles were formed a stratified bed as a given composition in the pyrex tube to a certain height. Calibration of the heat generation rate in the particulate bed as a function of generator

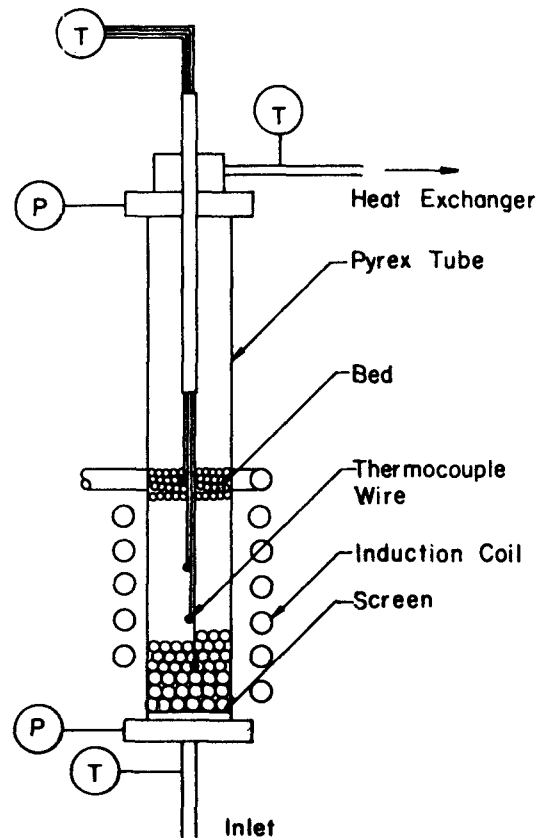


Fig. 2. Schematic Presentation of Test Section

power setting was made with measuring the temperatures at inlet and outlet of flow, and flow rate of the coolant through a bed for each run.

The tests were conducted according to the following procedure:

- (1) Turn on the pump and adjust the valves to have a desired flow rate and inlet temperature while turning on the induction heater for warming-up.
- (2) The power was increased in steps. At each power setting, time was allowed enough so that the dryout of the bed would occur if the heat generation rate was high enough.
- (3) Dryout of the bed was observed visually by glowing as well as by noting the sharp rise in the temperature of one or more of the thermocouples.
- (4) Power was turned off after dryout was

Table 1. Composition of Stratified Bed (Volume Fraction, %).

Particle dia (mm)	1.50	2.50	3.00	4.00	5.00
Bed					
A	10	—	20	30	40
B	20	—	10	40	30
C	30	—	40	10	20
D	40	—	30	20	10
E	30	30	20	20	—
F	40	30	20	10	—

Table 2. Mean Particle Diameter and Porosity of Stratified Beds.

	A	B	C	D	E	F
Surface Area	4.065	3.871	3.261	3.026	2.743	2.484
Mean Dia. (mm)						
Arithmetic	3.910	3.665	3.022	2.789	2.599	2.355
Mean Dia. (mm)						
Equivalent	3.419	3.000	2.463	2.248	2.272	2.069
Dia. (mm)						
Porosity	0.400	0.396	0.389	0.386	0.381	0.380

observed. the observation was repeated at least once more under the same test conditions.

- (5) Repeat steps 1 through 4 under different test conditions.

Six compositions of stratified bed were chosen as shown in Table 1.

As the average particle diameter of the stratified bed, the surface area mean diameter, the arithmetic mean diameter, and the equivalent diameter are considered as follows.

Surface area mean diameter:

$$\bar{d} = [\sum f_i d_i^2]^{1/2} \quad (1)$$

Arithmetic mean diameter:

$$\bar{d} = \sum f_i d_i \quad (2)$$

Equivalent diameter:

$$d_{eq} = [\sum f_i / d_i]^{-1} \quad (3)$$

where f_i is the mass fraction of the size component d_i . The mean particle diameters and the measured porosity for each stratified bed were listed in Table 2.

3. Results and Discussion

The power density distribution within the bed was obtained by heating the dry bed and comparing the heating up rate at the different spatial positions, and it was found that the distribution had similar form with the previous work.³⁾

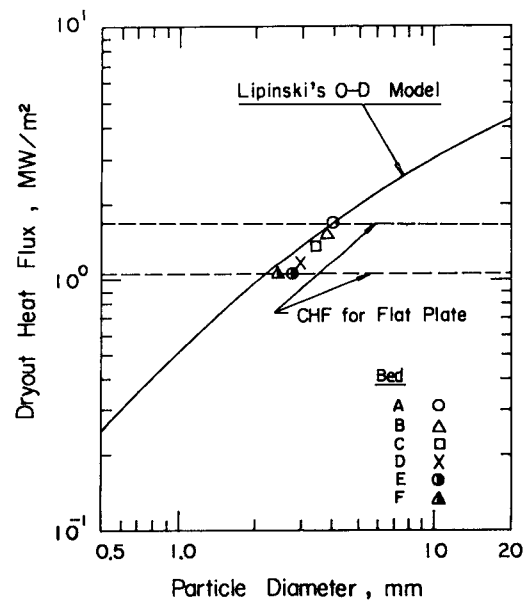


Fig. 3. Dryout Heat Flux vs. Particle Diameter at Zero Mass Flux based on Surface Area Mean Diameter

Through the visual observations, it was observed that dryout phenomena occurred frequently in the upper one-third region, especially at the boundary surface between top layer and second layer from the top. And there was no channeling appeared at the top of the bed.

During the tests, dryout heat fluxes at zero mass flux were measured with six stratified beds for 110 mm bed height and 13°C inlet temperature of coolant. Figure 3 shows the influence of particle size based on the surface area mean diameter on the dryout heat flux is increasing with increasing

Table 3. Experimental Data

Mass Flux kg/m ² .s	Dryout Heat Flux (MW/m ²)					
	A	B	C	D	E	F
0	1.650	1.322	1.242	1.183	0.990	1.070
0.35	1.832	1.507	1.398	1.378	1.187	1.340
0.70	2.216	1.903	1.756	1.663	1.331	1.701
1.40	2.540	2.380	2.169	2.131	1.837	1.924
2.10	2.594	2.455	2.362	2.148	2.232	2.101
2.80	2.889	2.661	2.498	2.440	2.421	2.404
3.50	—	2.918	—	—	—	—

particle size as previous investigators observed. It appears that Lipinski's mode⁴⁾ predicts in a good agreement with measured data.

All the data are listed in Table 3 and are plotted in figure 4 as a function of mass flux. As shown in Figure 4, the dryout heat flux in the stratified bed increases with an increase in mass flux. A similar trend of an increasing rate of dryout heat flux in the stratified bed was observed in the uniform particle size bed. Theoretically, the dryout heat flux asymptotically approaches total evaporation energy,

$$w(h_{fg} + c_{pf} \Delta T_{sub}),$$

where

w = mass flux

h_{fg} = heat of evaporation

c_{pf} = specific heat of coolant

ΔT_{sub} = subcooling of inlet coolant.

In the lower mass flux region, the dryout heat flux approaches the total evaporation energy of the inlet flow; higher than 1 kg/m².s, the dryout heat flux is much lower than the value of the total evaporation energy. It means that all the inlet liquid is not evaporated when the dryout phenomenon occurs in the bed. It should be noted that there is some carry-over liquid flow in the outflow of bed even it appears the dryout phenomenon. In this tests, it was found that the ratio of the carry-over flow rate to the total flow increased with increasing of coolant mas flux as shown in Table 4.

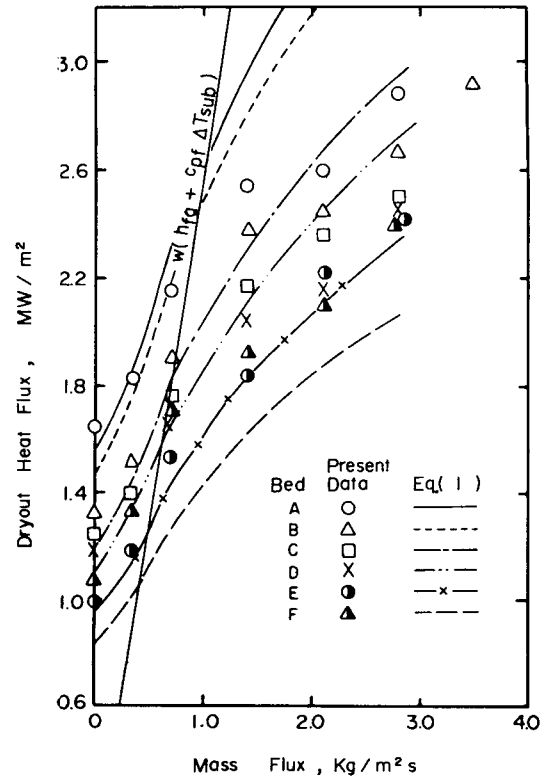


Fig. 4. Comparison of Experimental Data and Prediction based on Surface Area Mean Diameter

Table 4. Ratio of Carry-Over Flow to Total Flow.

Mass Flux kg/m ² .s	A	B	C	D	E	F
0.35	-0.99	-0.64	-0.52	-0.50	-0.29	-0.46
0.70	-0.18	-0.04	0.04	0.09	0.27	0.07
0.40	0.31	0.35	0.41	0.42	0.50	0.47
2.10	0.53	0.55	0.57	0.61	0.59	0.62
2.80	0.60	0.64	0.60	0.67	0.67	0.67
3.50	—	0.68	—	—	—	—

In a previous study,³⁾ the following form was chosen for an empirical formula for forced flow dryout heat flux;

$$q_{dw} = 1.73 w^{0.35} q_{do} \quad (4)$$

where

q_{dw} = forced flow dryout heat flux (W/m²)

w = coolant mass flux (kg/m².s)

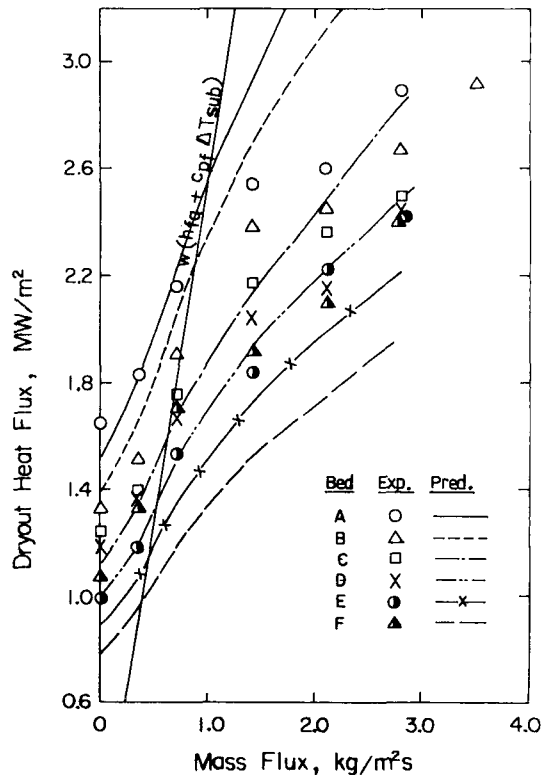


Fig. 5. Comparison of Experimental Data and Prediction based on Arithmetic Mean Diameter

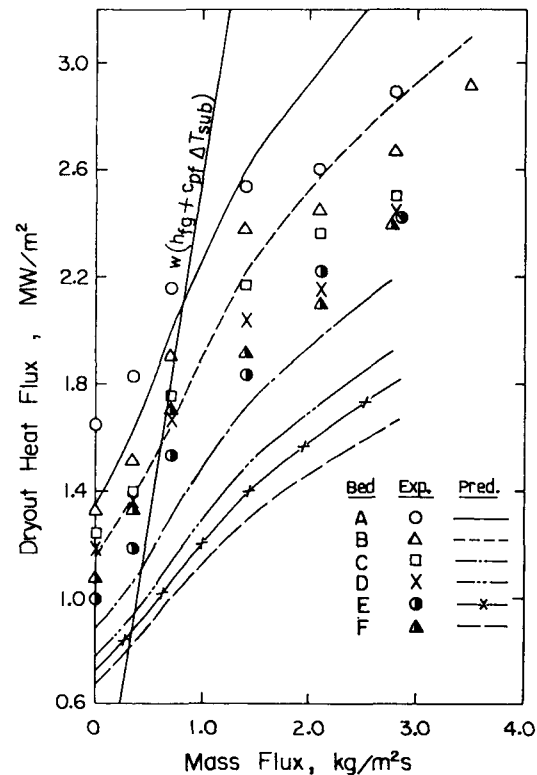


Fig. 6. Comparison of Experimental Data and Prediction based on Equivalent Diameter

q_{do} = dryout heat flux at zero mass flux (W/m^2)

and q_{do} can be obtained using Lipinski's zero-dimensional model.⁴⁾ Figure 4 also shows the comparison of present data and Equation (4) based on the surface area mean diameter.

Figure 5 and 6 also show the comparisons of the experimental data and empirical formula based on arithmetic mean diameter and equivalent diameter, respectively. Compared with above three figures, the use of surface area mean diameter as a particle diameter for the stratified bed was suitable for the calculation of dryout heat flux.

Figure 7 shows the comparison of experimental data and Lipinski's one-dimensional model predictions⁵⁾ based on surface area mean diameter of the particles. In the region of mass flux between 0 and 1 $kg/m^2.s$, Figure 7 indicates that Lipinski's one-dimensional model predicts the

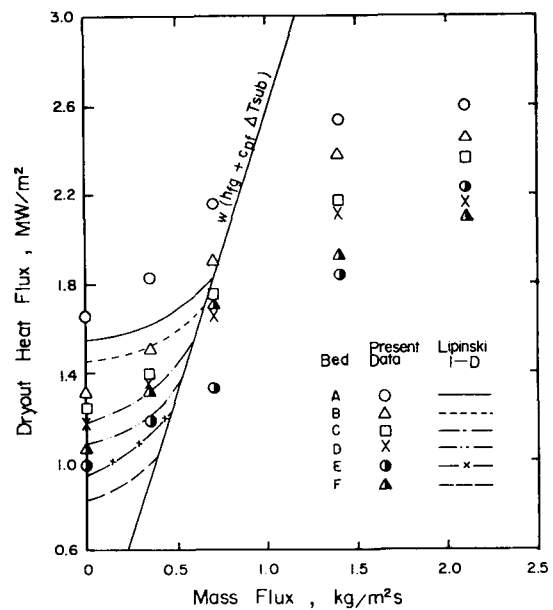


Fig. 7. Comparison of Experimental Data and Lipinski's 1-D Model based on Surface Area Mean Diameter

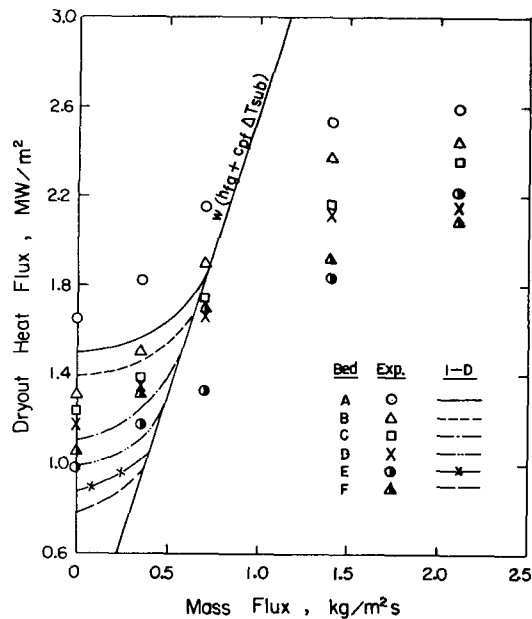


Fig. 8. Comparison of Experimental Data and Lipinski's 1-D Model based on Arithmetic Mean Diameter

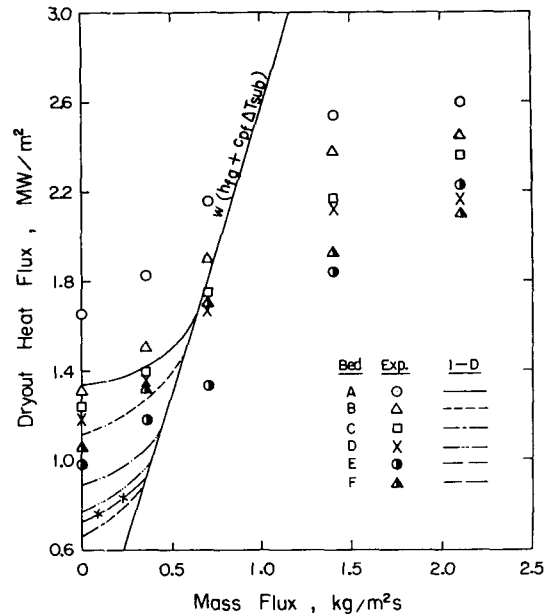


Fig. 9. Comparison of Experimental Data and Lipinski's 1-D Model based on Equivalent Diameter

data trend and magnitude well. Beyond $1 \text{ kg/m}^2 \cdot \text{s}$ mass flux, however, the trend of an increasing rate of dryout heat flux deviates extremely from both Lipinski's curve and the total evaporation energy curve. This was mainly attributed to the large amount of carry-over flow in the higher mass flux region.

Figures 8 and 9 show the comparisons of experimental data and Lipinski's 1-D model predictions based on the arithmetic mean diameter and the equivalent diameter, respectively.

There was only one existing work on flow boiling dryout in the stratified debris bed, i.e. the DCC-3 experiment.²⁾ Because of different test conditions, it is something hard to get the comparison between the present and DCC-3 data. The typical dryout heat flux data with the stratified bed of DCC-3 were as follows: 1.313 MW/m^2 with $0.5 \text{ kg/m}^2 \cdot \text{s}$, 0.666 MW/m^2 with $0.25 \text{ kg/m}^2 \cdot \text{s}$, and 0.323 MW/m^2 with $0.175 \text{ kg/m}^2 \cdot \text{s}$, under the conditions of 166°C inlet temperature and 0.718 MPa system pressure. It can be found that the dryout heat flux is almost directly proportional

to the inlet mass flux. Generally the values of dryout heat fluxes in DCC-3 with the mass flux were much lower than the present data, especially in lower mass flux. It seems that these lower values were attributed to the shape and the ingredient of particles used in the tests. However, the highest value of dryout heat flux in DCC-3, 1.313 MW/m^2 with $0.5 \text{ kg/m}^2 \cdot \text{s}$ is comparable with the value for the B bed of present work.

4. Conclusions

Test results dictated the following conclusions:

1. The dryout heat flux in the stratified debris bed increases with upward forcing mass flux. The similar trend of increase rate of dryout heat flux in the stratified bed was observed in the uniform particle size bed. In the lower mass flux region, less than $1 \text{ kg/m}^2 \cdot \text{s}$, the dryout heat flux approaches the total evaporation energy of the inlet flow, however, in the higher mass flux region, greater than $1 \text{ kg/m}^2 \cdot \text{s}$, the dryout heat flux is much lower than the values of total evaporation energy.

poration energy.

2. For the comparison of theoretical values and experimental data, the use of surface area mean diameter as a particle diameter was suitable for the calculation of dryout heat flux.
3. It was found that there were great deviations of forced flow dryout heat fluxes between experimental and Lipinski's 1-D model when the mass flux exceeds $1 \text{ kg/m}^2\text{s}$.

Acknowledgment

The authors wish to thank Mr. Soon Yeun Won for his assistance in providing the experimental setup.

References

1. D. Squarer, A. T. Piezynski, and L. E. Hochreiter, "Effect of Debris Bed Pressure, Particle Size, and Distribution on Degraded Nuclear Reactor Core Coolability", Nucl. Sci. eng., vol. 80, pp. 110-113, 1981.
2. K. R. Boldt, A. W. Reed, and T. R. Schmidt, "DCC-3 Degraded Core Coolability: Experiment and analysis", USNRC Report, Sandia National Laboratory, April 1986.
3. J. H. Cha, M. K. Chung, "Forced Flow Dryout Heat Flux in Heat Generating Debris Bed," J. Kor. Nucl. Soc., vol. 18, p. 273, 1986.
4. R. J. Lipinski, "A Particle-Bed Dryout Model with Upward and Downward Boiling," Trans. Am. Nucl. Soc., vol. 35, p. 358, 1980.
5. R. J. Lipinski, "A Coolability Model for Postaccident Nuclear Reactor Debris," Nucl. Technol., vol. 65, p. 53, 1984.